



Cite this: *RSC Adv.*, 2022, **12**, 19122

Received 27th April 2022  
 Accepted 21st June 2022

DOI: 10.1039/d2ra02674k

rsc.li/rsc-advances

## A short review on the synthesis and advance applications of polyaniline hydrogels

Aleena Mir,<sup>a</sup> Amit Kumar<sup>b</sup> and Ufana Riaz<sup>b</sup>   <sup>\*a</sup>

Conductive polymeric hydrogels (CPHs) exhibit remarkable properties such as high toughness, self-recoverability, electrical conductivity, transparency, freezing resistance, stimulus responsiveness, stretch ability, self-healing, and strain sensitivity. Due to their exceptional physicochemical and physio-mechanical properties, among the widely studied CPHs, polyaniline (PANI) has been the subject of immense interest due to its stability, tunable electrical conductivity, low cost, and good biocompatibility. The current state of research on PANI hydrogel is discussed in this short review, along with the properties, preparation methods, and common characterization techniques as well as their applications in a variety of fields such as sensor and actuator manufacturing, biomedicine, and soft electronics. Furthermore, the future development and applications of PANI hydrogels are also mentioned.

### 1 Introduction

Hydrogels are 3D cross-linked network architectures of hydrophilic polymer chains having remarkable water holding capacity.<sup>1–5</sup> The interaction between polymeric chain networks and water/biological fluids results in the formation of hydrogels through the entanglement of interpenetrated, osmotic, and hydration forces, which are counter-balanced, causing chain network expansion.<sup>6–8</sup> The amplitude of these opposing effects determines the equilibrium state of the hydrogel, which dictates several inherent qualities of the hydrogel, such as internal transport, diffusion characteristics, and mechanical strength. Tunable and reversible physical/chemical properties, stimuli-responsiveness, biomimetic, and biocompatibility are the key features of hydrogels.<sup>9–11</sup> As a result, these materials have proven to be effective in a variety of advanced technological applications.

Conducting polymers (CPs) have gained a lot of attention over the last few decades because of their unique ability to exhibit electrical conductivity due to the presence of extended  $\pi$  conjugation.<sup>12–14</sup> CPs are intrinsically inflexible and display great stiffness because of their conjugated structure. Conductive polymeric hydrogels (CPHs) are a new class of polymeric materials that combine the advantages of organic conductors and hydrogels.<sup>15</sup> These gels exhibit remarkable synergistic ability which combines the swelling behaviour of traditional hydrogels as well as electro-activity comparable to that of semiconductors.<sup>16</sup> They also show sensitivity towards changes

in pH, temperature, external stress, electric field, *etc.* and serve as an ideal interface between electronic (electrode) and ionic (electrolyte) transport phases under natural and synthetic biological systems.<sup>17</sup> Various strategies have been employed to control the properties of these hydrogels by incorporation of multi-functional groups so as to widen their applications in 3-D printing, self-healing,<sup>18</sup> functional response,<sup>19</sup> controlled stimuli-responsive drug delivery systems,<sup>20</sup> wearable sensors,<sup>21</sup> and adsorption of dyes.<sup>22</sup> CPHs have also been utilized in designing energy storage devices,<sup>23</sup> microbial fuel cells,<sup>24</sup> and molecular/bioelectronics devices.<sup>25</sup>

Among the several conducting polymers, polypyrrole (PPy),<sup>26</sup> polythiophene (PTh),<sup>27</sup> polyethylenedioxy thiophene (PEDOT),<sup>28</sup> polyaniline (PANI)<sup>29</sup> has been extensively investigated due to its ease of processibility, the ability to exist in various redox forms. Lately, PANI has been widely explored for its potential application as a supercapacitor and also in designing microbial fuel cells.<sup>30–34</sup> Keeping in view the popularity of PANI and its advance applications in various fields, the present review discusses synthetic strategies adopted to design PANI based hydrogels. The chemical as well as electrochemical methods adopted to design PANI and PANI composite hydrogels are highlighted along with their potential applications in environmental as well as biological fields.

#### 1.1 Brief survey of publications on PANI hydrogels

PANI hydrogels have been widely synthesised by electrochemical and chemical methods. Approximately 503 publications are available on PANI hydrogels in the year 2021 with a total of 5386 citations.<sup>29</sup> Among the disciplines, almost 185 articles are published under Materials Chemistry discipline, while 135 articles are published under Physical Chemistry

<sup>a</sup>Materials Research Laboratory, Department of Chemistry, Jamia Millia Islamia, New Delhi-110025, India. E-mail: uriaz@jmi.ac.in; ufana2002@yahoo.co.in

<sup>b</sup>Theory & Simulation Laboratory, Department of Chemistry, Jamia Millia Islamia, New Delhi-110025, India. E-mail: akumar1@jmi.ac.in



category and around 76 articles are available under the nanoscience/nanotechnology category, Fig. 1.

## 1.2 Synthesis of PANI hydrogels

The incorporation of PANI into the hydrogel matrix allows for the enhancement of hydrogel elasticity, swelling ratio, and electrochemical response of the gel towards the environment which facilitates transport of nutrients, drugs, and metabolites.<sup>17</sup> The chemical method involves the polymerization of the aniline monomer in a hydrogel matrix. This technique is further classified into two methods. The first method deals with *in situ* polymerization of aniline in a prefabricated hydrogel, while the second method involves mixing of monomers of conducting polymers and hydrophilic polymers followed by either step wise or simultaneous addition of cross linker. The electrochemical technique deals with the deposition of aniline by applying a suitable potential on hydrogel films which are used as working electrode for the electrochemical polymerization of aniline. The techniques are discussed in detail in the proceeding sections.

**1.2.1 Chemical polymerization of conducting monomer in a prefabricated hydrogel.** PANI (emeraldine base) was successfully incorporated into a pre-made hydrogel by Martinez *et al.* (2015)<sup>35</sup> from its solution in *N*-methylpyrrolidone (NMP), Fig. 2. These CPHs were homogeneous in nature, with a uniform distribution of the emeraldine base's blue colour throughout the hydrogel matrix. The hydrogel was then acid-treated to convert the emeraldine base to emeraldine salt. The volumes phase transition temperature was increased and the existence of PANI improved the mechanical properties but the electric properties were dependent on the external pressure applied. The electrical resistance decreased about 5 k $\Omega$  for 10% of compression.

In 2011, Molina *et al.*,<sup>36,37</sup> developed a hydrogel by utilizing PANI stabilised in polyvinylpyrrolidone (PVP) forming an interpenetrating network with poly(*N*-isopropylacrylamide). The influence of conducting polymer interpenetration on the thermo-sensitivity, swelling and ion exchange governed the macro properties of hydrogels. Moreover it was observed that the incorporation of PANI could be used to alter the properties of hydrogels, ignoring their conducting properties. Wu *et al.*,<sup>38</sup> utilized poly(ethylene glycol) diacrylate hydrogel (PEGDA) and PANI was cross-linked with the polymer *via* interfacial polymerization. It was noticed that there was an insignificant change in the mass swelling and compressive modulus of PEGDA/PANI samples as compared to pure PEGDA which could be used to develop biomimetic electrical interfaces. Huang *et al.*,<sup>39</sup> developed CPHs comprising of aniline which was polymerized *in situ* in a solution of sodium alginate, which exhibited an electrical conductivity of  $10^{-3}$  S cm $^{-1}$ . The hydrogels revealed high specific capacitance, a low resistance, and a good cycling stability which were proposed to be used as electrode materials for supercapacitors. Nourbakhsh *et al.*,<sup>40</sup> developed an injectable electroactive hydrogel of pluronic-chitosan/aniline pentamer with conductivity around  $10^{-4}$  S cm $^{-1}$ , while Rahman *et al.*<sup>41</sup> used prefabricated chitosan films and polymerized aniline using ammonium persulphate (APS) as an oxidant and sodium phytate as dopant. Chitosan served to be beneficial as a substrate due to its malleability, mechanical strength which did not hamper the electrical property of PANI and was proposed to be helpful for the utilization of polymeric patches in tissue engineering.

This strategy of *in situ* polymerization of conducting monomer in a prefabricated hydrogel is commonly used to prepare conductive hydrogels for biomedical applications. The key

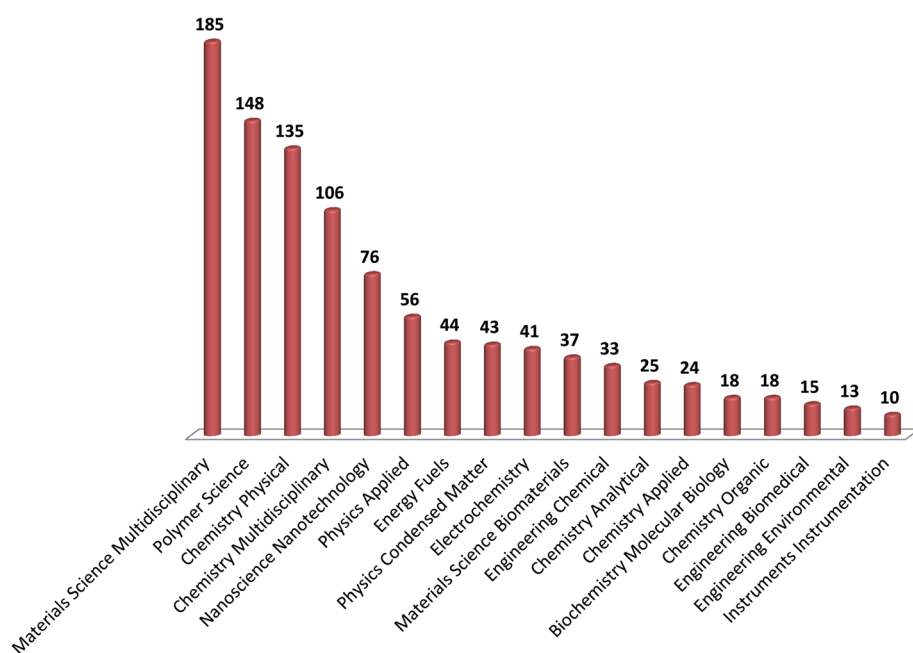


Fig. 1 Papers published on PANI gels in various disciplines.



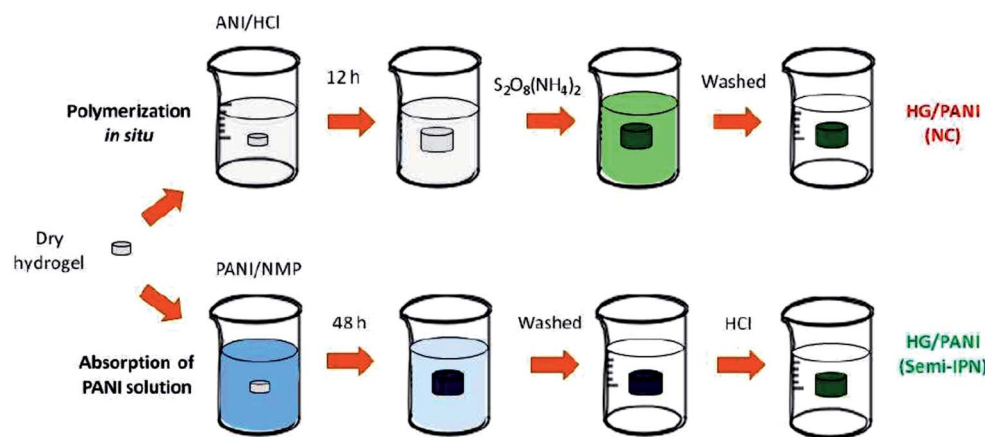


Fig. 2 Schematic representation of the semi-interpenetration steps to load PANI inside PNIPAM-co-2%AMPS hydrogel matrix by two different methods. (Reprinted with permission from Elsevier, ref. 35 Martinez *et al.* (2015)).

advantages of this method are homogeneous *in situ* polymerization of conductive polymers in the presence of uniform oxidants, as well as the attainment of an acceptable level of solubility in the hydrogel matrix.

**1.2.2 Mixing of monomers of conducting polymers and hydrophilic polymers followed by either step wise or simultaneous addition of cross linker.** This technique is also regarded as the easiest and simplest approach for the synthesis of PANI based hydrogels. The *in situ* polymerization of aniline was carried out by grafting aniline to quaternized chitosan followed by the addition of oxidized dextran as a Schiff crosslinker to form a conductive hydrogel network by Zhao *et al.*<sup>42</sup> The hydrogel exhibited a conductivity of  $0.43 \text{ mS cm}^{-1}$  and was reported to maintain cell viability and promote cell proliferation. Sharma *et al.*<sup>43</sup> Synthesised a cross-linked hydrogel using a solution of aniline and poly(sodium 4-styrenesulfonate), *via* irradiation technique Fig. 3. The electrical conductivity

increased with an increased concentration of 1.5 N HCl but at higher concentrations, a decrease in electrical conductivity was noticed due to over protonation of PANI.

Dai *et al.*<sup>44</sup> used an interfacial polymerization technique to create a PANI hydrogel utilising polyacrylamide (PAAm). PANI hydrogel was synthesised using phytic acid as cross linker and dopant. The electrical conductivity was measured to be  $2.1 \times 10^{-2} \text{ S cm}^{-1}$  which was higher than the hydrogel prepared *via* conventional sequential process. Ji *et al.*<sup>45</sup> developed graphene/PANI composites by chemical oxidative polymerization of aniline in the presence of graphene oxide with phytic acid as a cross-linker. The hydrogels were utilized as additive-free supercapacitor electrodes, exhibiting specific capacitance as high as  $1217.2 \text{ F g}^{-1}$  (scan rate of  $10 \text{ mV s}^{-1}$ ) at the current density of  $1 \text{ A g}^{-1}$  in an aqueous electrolyte of  $1 \text{ M H}_2\text{SO}_4$ . When aniline and *o*-phenylenediamine were copolymerized in presence of PAAm, a hydrogel was formed.<sup>46</sup> The CP grafted PAAm

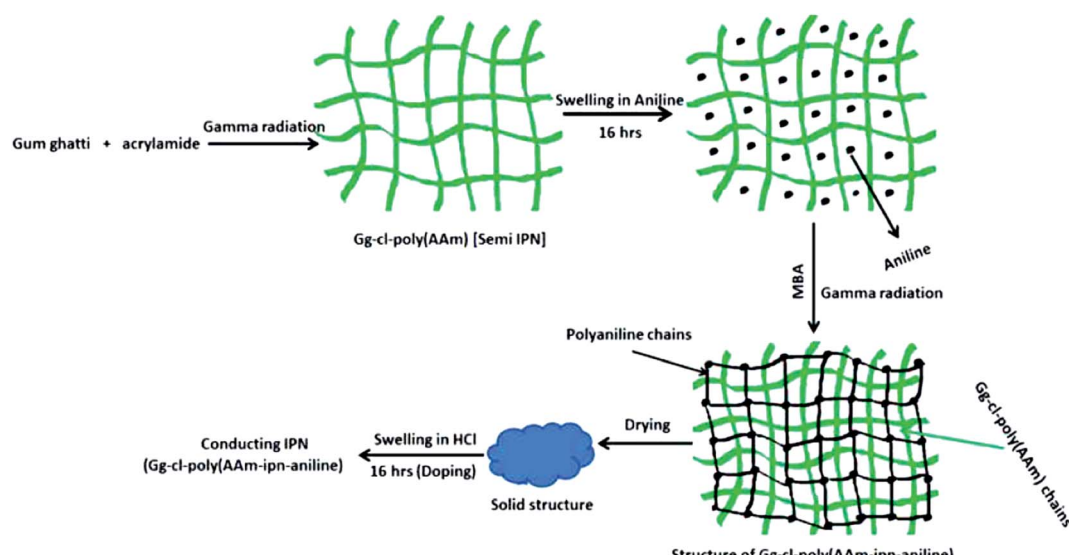


Fig. 3 Mechanism of radiation induced polymerization process. (Reprinted with permission from Elsevier, ref. 43 Sharma *et al.* (2014)).



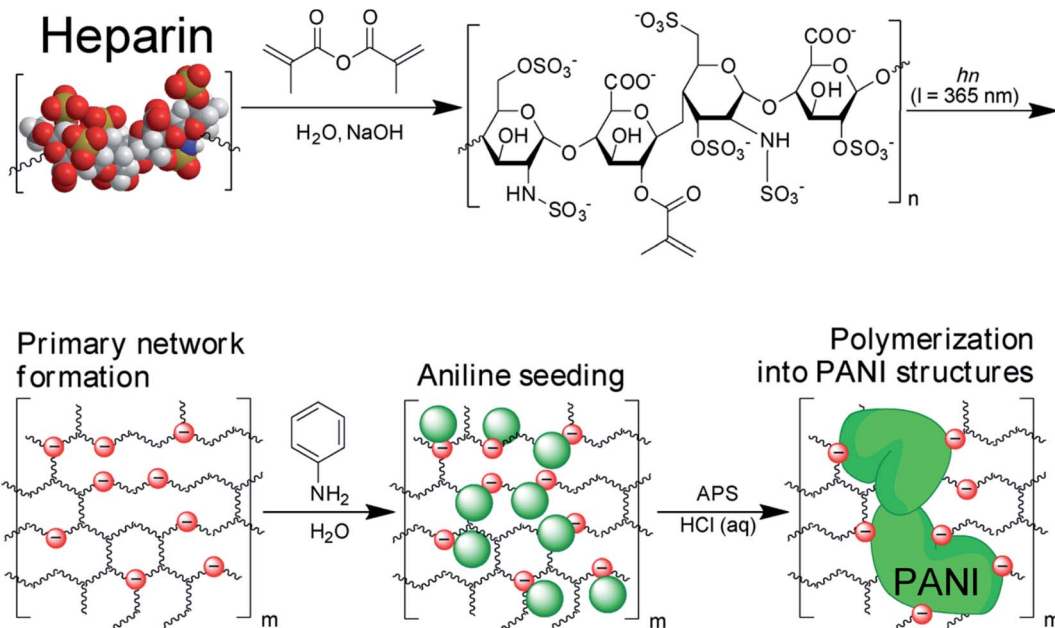


Fig. 4 Synthetic scheme of Hep-MA/PANI hydrogel dual networks. Photo-cross-linkable heparin was prepared via conjugation with methacrylate groups. Primary heparin gel networks were formed through photo-cross-linking of heparin-methacrylate (Hep-MA) at UV wavelengths ( $\lambda = 365$  nm). Hep-MA gels were then loaded with ANI monomers, which were then converted into PANI structures via *in situ* oxidative polymerization. (Reprinted with permission from American Chemical Society, ref. 47 Ding *et al.* (2014)).

hydrogel was utilized as pseudo-supercapacitor electrode showing a maximum capacitance value of  $364 \text{ F g}^{-1}$  at  $0.2 \text{ A g}^{-1}$ .

Ding *et al.*<sup>47</sup> synthesised flexible and stretchable heparin-doped PANI hydrogel, Fig. 4 using Heparin-methacrylate (Hep-MA) as the primary network precursor, which was cross-linked via photoinduced free radical polymerization. The anionic *in situ* polymerization of aniline was then carried out to form electrically conductive hydrogels composed of Hep-MA/PANI dual networks. The redox behavior and DC conductivity based on  $Z'(Re)$  of  $600 \Omega$  at  $\omega = 0.01 \text{ Hz}$  was comparable to published literature and Hep-MA/PANI networks showed outstanding mechanical properties which permitted myoblast adhesion and differentiation. A simple oxidative approach was used to make chitosan-*graft*-PANI copolymers by Marcasuzaa *et al.*<sup>48</sup> PANI hydrogel was chemically synthesised by using *p*-toluenesulfonic acid as dopant and APS as oxidant. The conductivity was reported to be in the range of  $10^{-2} \text{ S cm}^{-1}$  and the gels were found to act “superabsorbent” showing reversible swelling properties. Guarino *et al.*<sup>49</sup> synthesised PANI hydrogel through chemical oxidative polymerization using poly(ethylene glycol) diacrylate (PEGDA) as network agent for nerve generation. The loading of PANI up to 3 wt% exhibited an electrical conductivity of  $1 \times 10^{-3} \text{ S cm}^{-1}$ . The presence of PANI also improved the water retention/proton conductivity by more than one order of magnitude. MWCNTs and PANI hydrogel were designed by Yang *et al.*<sup>50</sup> to form an anode with a high areal capacitance of  $2434.7 \text{ mF cm}^{-2}$ . The hydrogel framework showed continuous transport pathways for electrons/electrolyte ions in the electrode system besides low resistance. Nath *et al.*<sup>51</sup> formulated a multi-walled carbon nanotube (MWCNT) based PANI/PVA hydrogel via *in situ* polymerization of aniline in a mixture of

PVA and MWCNT, which was used as dye-sensitized solar cells (DSSCs). The addition of MWCNT enhanced the electrical characteristics by enabling the charge transfer of electrolytes and a maximum energy conversion efficiency of 2.18% was attained upon loading of 0.75% MWCNT. Liu *et al.*<sup>52</sup> developed a composite hydrogel based on poly(acrylamide-*co*-sodiummethacrylate)/PANI/carboxylfunctionalized multi-walled carbon nanotubes (PAM-*co*-SMA)/(PANI/MWCNTs-COOH). The lower loading of PANI showed better swelling capability, good swelling reversibility, higher pH sensitivity, higher compressive strength and good strain recoverable ability due to better dispersion at lower loadings. Wang *et al.*<sup>53</sup> designed PANI based reduced graphene oxide (rGO) composite hydrogel through one-step synthesis in which iodine was used as a catalyst as well as dopant. The hydrogel exhibited specific capacitance of  $712.5 \text{ F g}^{-1}$  at a current density of  $1 \text{ A g}^{-1}$  and could be utilized in high performance storage devices. Taşdelen<sup>54</sup> adopted free radical solution polymerization technique to develop PAAm/kaolin composite hydrogel. The kaolin particles were embedded within the network PAAm hydrogel in which aniline monomer was absorbed and polymerized at room temperature to create a unique semi-interpenetrating network (semi-IPN). The conductivity of the semi-IPN was found to be  $1.1 \times 10^{-4} \text{ S cm}^{-1}$ . Temperature responsive and electrically conductive porous poly(*N*-isopropylacrylamide)/SiO<sub>2</sub>/PANI hydrogels were synthesized by Depa *et al.*<sup>55</sup> The synthesis was carried out via two step method and the impregnation of porous SiO<sub>2</sub> precursor gel with PANI precursor resulted in highly selective incorporation of PANI into the pore walls of SiO<sub>2</sub>. The percolation threshold of PANI was attained near 20 wt%, and 44 wt% which also provided distinct mechanical reinforcement



in the composite hydrogels. Chen *et al.*<sup>56</sup> developed MWCNT based PANI hydrogel using phytic acid as a dispersing agent and gelator in an aqueous MWCNT solution containing aniline. The hydrogels showed electrical conductivity ranging between 0.21 and 1.54 S cm<sup>-1</sup> as the loading of MWNTs increased from 0 to 5.0 wt%. A maximum specific capacity of 609 F g<sup>-1</sup> was reported for the hydrogels containing 3 wt% MWNT loading. Zhang *et al.*<sup>57</sup> adopted cryopolymerization method for preparing intrinsically stretchable anisotropic PVA/PANI hydrogel. The electrodes exhibited a specific capacitance of 260 F g<sup>-1</sup> and 650 mF cm<sup>-2</sup> and a high energy density of 27.5 W h kg<sup>-1</sup> along with excellent stability under the harsh stretching, compressing, and bending operations.

### 1.2.3 Electrochemical polymerization of PANI hydrogels.

The electronic conductivity of PANI is governed by the extent of conjugation which arises due to the presence of  $\pi$ -bonds and strongly localized  $\sigma$ -bonds. During electro-polymerisation, the  $\pi$ -bonds overlap each other generating electron redistribution and the delocalized electrons are allowed to move freely within the polymeric backbone, inducing electronic conductance. Hence for the purpose of achieving high electrical conductivity in PANI based hydrogels, the electrochemical method of polymerization has been adopted particularly for fabricating as PANI electrodes for their utilization as microbial fuel cells, supercapacitors, dye sensitized solar cells *etc.* Dmitriev *et al.*<sup>58</sup> formulated PANI/PAAm hydrogels *via* polymerization of aniline in the PAAm solution in acetone. The composite gels showed swelling in water, acid and base solutions and dimethyl sulfoxide and demonstrated the elastic response like a covalently cross-linked network providing mechanical integrity, good-quality mechanical response, swelling ability and electrical characteristics. The hydrogel was created electrochemically on the electrode surface through electro polymerization, which improved electrode conductivity. Lira *et al.*<sup>59</sup> designed PANI/PAAm hydrogels *via* electro-polymerization of the aniline monomer inside the polyacrylamide hydrogel matrix. The electro-mechanic properties of PANI aided the drug release of safranin *via* an electric pulse which was governed by the oxidation state of PANI in the polymer hydrogel composite. Wang *et al.*<sup>60</sup> utilized PANI hydrogel as an active electrode material to make a flexible solid-state supercapacitor with a capacitance value as high as 430 F g<sup>-1</sup>. This capacitance value was claimed to be the highest for a PANI based solid-state supercapacitor with two-electrode system.

Chu *et al.*<sup>61</sup> carried out electrochemical polymerization of aniline using phytic acid as cross linker and dopant to develop a three-dimensional (3D) supramolecular PANI based hydrogel. The conducting hydrogel was used as high performance flexible solid state capacitor (FSSC) and a high conductivity of 0.43 S cm<sup>-1</sup> was attained at room temperature. Due to enhanced electrode interfaces between electronic transporting phase and ionic transporting phase, a large areal capacitance of 561.6 mF cm<sup>-2</sup> and specific capacitance of 311.3 F g<sup>-1</sup> was achieved. Zhai *et al.*<sup>62</sup> developed glucose sensor using nanoparticles of platinum (PtNPs) and PANI hydrogel electrodes in which the PtNPs were densely loaded onto the hydrogel matrix. The PtNP/PANI hydrogel based glucose sensor exhibited sensitivity, as high as

96.1  $\mu$ A mM<sup>-1</sup> cm<sup>-2</sup> and a low detection limit of 0.7  $\mu$ M. Zeng *et al.*<sup>63</sup> utilized the electrochemical oxidation process using high-performance carbon nanotube (CNT) *via* floating catalyst chemical vapor deposition (FCCVD) method. The films exhibited high areal capacitance of 680 mF cm<sup>-2</sup>. Gao *et al.*<sup>64</sup> electrodeposited PANI on graphene hydrogel (GH) to improve the pseudo-capacitive effect and the energy density bodies maintaining the power capability. The composite hydrogel exhibited excellent specific capacitance of 710 F g<sup>-1</sup> at 2 A g<sup>-1</sup> and 73% capacitance retention and a maximum energy density of 24 W h kg<sup>-1</sup> along with power density and 30 kW kg<sup>-1</sup>.

The studies clearly reveal the enhancement in the properties of hydrogels upon insertion/grafting/incorporation of PANI. Based on the homogeneity and deposition technique adopted to formulate the hydrogels, superior capacitance and electrical properties have been achieved. However the morphology and rheological properties are also important in characterizing the hydrogel and hence, the upcoming section discusses the fundamental characterization techniques and their significance in exploring the performance of PANI based conductive hydrogels.

### 1.3 Characterization techniques adopted for exploring the properties of hydrogels

CPHs shows some valuable and distinct properties like softness, plasticity, better mechanical strength than conventional polymers, high water content, porosity, high surface area specificity, electrical conductivity, redox activity and conversion among themselves into conducting and non-conducting forms.<sup>65,66</sup> The qualities, such as mixed electronic and redox activity, ionic conductivity, and responsivity, are easily integrated with material properties, such as mechanical integrity, biocompatibility, and elasticity, provided by supporting polymers. The structural determination and characterization of the cross-linked network formation is required for the creation of hydrogels with desired properties. Physical, spectroscopic, thermal, morphological, and mechanical approaches are commonly used to gain insight into the hydrogels' intricate structural intricacies, Fig. 5.

**1.3.1 Physico-chemical characterization.** One of the characteristic features of hydrogel is its swelling response when subjected to various environmental matrices such as pH, water. Swelling kinetics and equilibrium is affected by a number of factors including the ionic media, cross linker, chemical structure, temperature *etc.* Swelling of a hydrogel is measured in terms of swelling ratio of swollen gel to dry gel. One of the most crucial physical aspects of hydrogels is their soluble nature. This can be determined by calculating the insoluble component of a dried sample following immersion in deionized water for 24–48 hours at room temperature. The weight acquired after filtration by vacuum can also be used to determine the insoluble fraction of the hydrogel.

**1.3.2 Rheological measurements.** Rheology is concerned with determining the link between deformation/flow and applied stress. The structural types present in the system, such as association, entanglement, and cross-links, have a significant impact on the rheological study. Thus rheology provides an



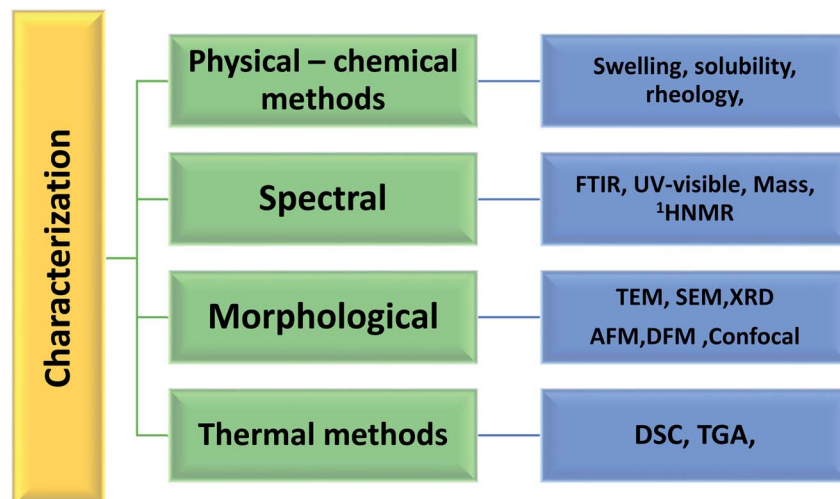


Fig. 5 Flow chart depicting characterization techniques of CPHs.

insight into the structural details of hydrogels. At low frequencies, polymer solutions become viscous, tending to follow the scaling rules G02 and G00. Elasticity prevails even at high frequencies ( $G_0 > G_{00}$ ). This is due to Maxwell-type behaviour, which has a single relaxation period that can be calculated from the crossover point and grows with concentration.

**1.3.3 Spectroscopic techniques.** Light absorption in the UV-Vis range can be used to discover specific chemical bonds in tiny molecules and polymers. In PANI hydrogels, it also aids in the detection of certain electronic transitions. Infrared spectroscopy is most extensively used approach for detecting the chemical structure of PANI based CPHs is infrared spectroscopy, which provides information on the numerous types of chemical bonds, the atoms involved, and the local chemical environment present within a material.<sup>67</sup> This strategy has a number of advantages, the most notable of which is its versatility in terms of sampling methodologies. Depending on the type of sample, the measuring mode is chosen. Mass spectroscopy is an analytical technique for determining the polymer's composition based on the mass-to-charge ratio of charged particles. MALDI stands for matrix-assisted laser desorption/ionization and is a soft ionisation technique for high-resolution mass spectroscopy of synthetic and biological macromolecules, as well as polymers. Various modes of NMR are also used to investigate PANI based hydrogels. Identification of functional groups of monomer and copolymer composition, completion of the polymerization process and verification of its mechanism, information on water molecule exchange between the free and bound states can be identified. Dynamic Light Scattering is extensively used for determining particle size, molecular dispersion, and characteristics.

**1.3.4 Morphological techniques.** X-Ray diffraction analysis helps in identifying the chemical properties of gels with varying "degrees of crystallinity" differ, which is commonly expressed as a crystallinity % or crystalline/amorphous ratio. The degree of crystallinity can also be easily evaluated using XRD. Electron microscopy is used to study the gel dispersions. When compared

to all other procedures, the main advantage of this technique is the ability to immediately watch the creation of inter-particle bridges. Secondary nucleation results in atypical particle production and the presence of smaller particles are also detected using this technique. These techniques can't be utilised to accurately measure a swollen gel. Furthermore, due to lowered pressure and electron beam irradiation, a swelling gel may aggregate. Scanning electron microscopy (SEM) gives information about the surface topography, shape, and composition of the hydrogels can all be determined using scanning electron microscopy. The swelled hydrogels are freeze-dried for 6 hours at 52 °C for morphological characterisation. The hydrogel's swelling behaviours, such as preliminary swelling and deswelling, can also be examined. It is possible to explore the effects of pH and inorganic salt on the swelling behaviour of PANI hydrogels.<sup>68,69</sup> The atomic force microscopy (AFM) is also a common technique that makes a topographic image of the hydrogel surface and provides information about its surface properties, while dynamic force microscopy (DFM) gives improved structural images of the polymer network structure after solvent extraction, as well as their relationship to the preferred system's improved swelling property in various environmental conditions such as as pH, solvent, and salt concentration, are displayed using the dynamic force microscopy technique.

**1.3.5 Thermal techniques.** Differential scanning calorimetry (DSC) can be used to determine the degrees of crystallinity and crystal size distributions of samples in their original state (before swelling) as well as during various phases of swelling. It also looks into the crystalline nature of hydrogels, especially those that have been frozen and thawed. The thermogravimetric analysis (TGA) helps to identify the rate at which thermal degradation occurs. The mass loss of the hydrogel appears to be linked to adsorbed water, as observed.

#### 1.4 Applications of PANI based hydrogels

According to a web of science research, biological applications of PANI-based hydrogels have been reported in 45% of



publications dealing with biomaterials Science over the last 22 years. The electrochemical properties of PANI hydrogels were mentioned in roughly 33% of the articles and almost 18% of the research has been published in journals of chemical engineering.<sup>29</sup>

**1.4.1 Biomedical applications.** The incorporation of PANI into the hydrogel matrix allows reduction of mismatch at the interface with biological cells and tissues, and the movement of nutrients, medicines, and metabolites. Injectable conductive interpenetrating polymer network (IPN) hydrogel with enhanced mechanical properties and good biocompatibility was synthesized by Li *et al.*<sup>68</sup> These hydrogels showed interpenetrating polymer network formation and could meet the required criteria for biomedical applications. PANI/PEGDA were developed by Komeri and Muthu<sup>69</sup> which were electro-conductive injectable single component hydrogels made from a fumarate-*co*-PEG-*co*-sebacate-*co*-macromer coupled with non-sulfonated/sulfonated PANI and PEGDA. The hydrogels were able to protect cells from oxidative stress comparable with ascorbic acid.

**1.4.2 Biosensors.** CPHs possess tenability, multi-responsive functionality and good biocompatibility as compared to conventional biosensor. They also exhibit ease of fabrication for *in vivo* sensing. Hence they have been a subject of extensive investigations particularly in the field of clinical diagnostics and real-time biomolecule sensors. Wang *et al.*<sup>70</sup> created a flexible conductive supramolecular polymer hydrogel (CSPH) based on PANI that was electrically conductive and also showed antifouling properties. The films were electro-polymerized to provide highly selective thrombin recognition. For enhancing detection sensitivity, signal amplification probes were created, and a sandwich-type electrochemical aptasensor was built using CSPH-based electrode interfaces. Yang *et al.*<sup>71</sup> synthesized conducting PANI/poly(styrene sulfonate) (PSS) in a one-step co-polymerization process and a low fouling hydrogel based biosensor was developed. With a wide linear range and a low sensing limit, the biosensor has demonstrated good sensing capability. Qing *et al.*<sup>72</sup> synthesised poly-4,8-bis[5-(2-ethylhexyl)thiophen-2-yl] to develop a photocathodic enzymatic biosensor. The biosensor was fabricated using benzo[1,2-*b*:4,5-*b'*] dithiophene-2,6-diyl-*alt*-3-fluoro-2-[(2-ethylhexyl) carbonyl] dithiophene-2,6-diyl-*alt*-3-fluoro-2-[(2-ethylhexyl) carbonyl] dithiophene-2, PANI hydrogel as electron transfer layer and thieno[3,4-*b*]thiophene-4,6-diyl (PTB7-Th) as donor-acceptor-type photoactive material. The xanthine oxidase (XOD)-guanine catalytic reaction was investigated with the photocathodic enzymatic biosensor, which showed a low limit of detection of around 0.02  $\mu$ M within a linear range of 0.1 to 80  $\mu$ M. Han *et al.*<sup>73</sup> discovered a new class of adaptable CPHs based on a borax-cross-linked polyvinyl alcohol (PVA) hydrogel system and conducting PANI@CNF (polyaniline-cellulose nanofiber) nano-complexes that combined the conductivity of PANI with the template characteristic of CNFs, Fig. 6.

The hydrogels showed good biocompatibility, moldability, pH sensitivity, thermo-reversibility, and a 15 second self-healing time. After 3000 cycles, the hydrogel-based electrode with a conductivity of  $5.2 \text{ S m}^{-1}$  had a maximum specific

capacitance of  $226.1 \text{ F g}^{-1}$  and capacitance retention of 74%. The incorporation of such noteworthy qualities enabled the as-prepared CPHs to be used in flexible, self-healing, and implantable electronic devices. An ultrasensitive and protein-resistant label-free amperometric immunosensing platform was developed by Zhao *et al.*<sup>74</sup> for carcinoma antigen-125 (CA125) based on redox PANI/polythionine hydrogel (PANI-PThi). The constructed immunosensor revealed high specificity, allowing it to detect CA125 in human serum.

**1.4.3 Drug delivery.** Gum Ghatti-*co*-poly(acrylic acid-aniline) (Gg-*co*-poly(AA-ANI)) was designed by Sharma *et al.*,<sup>75</sup> *via* grafting aniline onto Gg-*co*-poly(AA) chains in the presence of *N,N'*-methylene-bis-acrylamide (MBA) and ammonium persulphate (APS) as a cross-linker. The ability of the synthesised hydrogels to be used as a colon-specific drug delivery vehicle was tested using amoxicillin trihydrate as a model drug in various pH media. The medication absorption was shown to be better in the cross-linked hydrogel with highest percentage swelling. Pourjavadi and Doroudian<sup>76</sup> developed hydrogel compound *via* radical co-polymerization of acrylic acid on the backbone of hydrolyzed collagen modified with polycaprolactone in the presence of a cross linker and *in situ* polymerization of aniline was carried out to incorporate conductive nano-fiber pathways throughout the hydrogel matrix. The studies pertaining to conductive-stimuli drug release of hydrocortisone as a model drug suggested that this hydrogel acted as externally controlled drug delivery system that could be tailored to match the physiological processes. Qu *et al.*<sup>77</sup> developed hydrogels of chitosan-*graft*-PANI copolymer using oxidized dextran (OD) as a cross-linker. The “on-off” pulse release was achieved with required electro-responsive property and smart release with pH-responsive property was demonstrated using amoxicillin model drug. Tsai *et al.*<sup>78</sup> designed CPHs based on PVA cross-linked with diethyl acetamidomalonate using PANI as the conductive component. The CPHs were fabricated in the form of cylindrical devices for electro-actuable release of the indomethacin drug.

**1.4.4 Supercapacitors.** Supercapacitors are regarded as future energy storage devices owing to their high power density, fast charge/discharge rate, long cycle life, and low maintenance cost. PANI exhibits remarkable redox chemistry, high conductivity, high mechanical flexibility, light weight, eco-friendliness, facile synthesis, and low cost. Flexible supercapacitors made of PANI nanowire arrays were synthesized by Fu *et al.*<sup>79</sup> in a folded, flat, and twisted configuration, indicating that they have a lot of promise for use in flexible electrochemical energy storage system. Jia and co-workers<sup>80</sup> designed a novel hydrogel of N/S co doped carbon aerogel with a 3D linked supra-molecular architecture developed from a methyl blue-doped PANI hydrogel (MB-PHG) through polymerization and carbonization. The synthesized capacitors showed the potential to break through the over potential barrier to an ultrahigh operating voltage window of 2.0 V, resulting in a high energy density of  $59.7 \text{ Wh kg}^{-1}$  at  $1 \text{ kW kg}^{-1}$ . Blade-coating and 3D printing was used to construct and prepare a double-network hydrogel electrode for use in an all-solid-state super-capacitor. Furthermore, the active material composition of the hydrogel electrode was



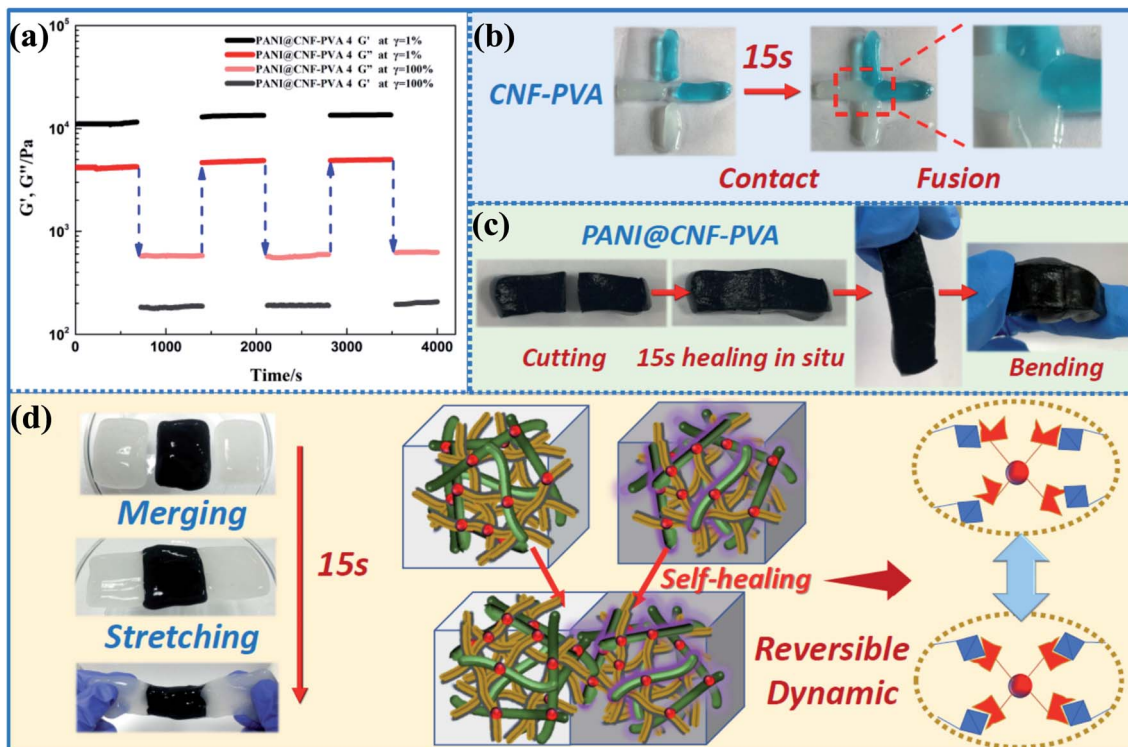


Fig. 6 (a) The  $G'$  and  $G''$  curves of PANI@CNF-PVA 4 as a function of time in continuous step strain tests. (b) Illustration of self-healing property for CNF-PVA and (c) PANI@CNF-PVA hydrogels. (d) Illustration of self-healing process of PANI@CNF-PVA and CNF-PVA hydrogels, and the self-healing mechanism of composite hydrogels with reversible network. (Reprinted with permission from Elsevier, ref. 73 Han *et al.* (2018)).

extraordinarily high (25.0 wt%), resulting in high area specific capacitance ( $871.4 \text{ mF cm}^{-2}$ ) and area energy density ( $0.14 \text{ mW h cm}^{-2}$  at  $0.27 \text{ mW cm}^{-2}$ ). Sol-gel and freeze-dried processes are used to create a new Ti3C2Tx/polyvinyl alcohol (PVA) porous sponge with 3D linked structures by Cao *et al.*<sup>81</sup> The manufactured PANI@Ti3C2Tx/PVA hydrogel composite is employed as flexible supercapacitors electrodes, and the Ti3C2Tx/PVA porous sponge is used as the template for *in situ* polyaniline (PANI) polymerization. Using *in situ* oxidative polymerization of aniline in the presence of MWCNT and phytic acid, a PANI/MWCNT composite hydrogel was effectively produced on carbon cloth, by Sardana and co-workers<sup>82,83</sup> which was used as a binder-free electrode for supercapacitors. For an efficient charge storage system, the 3D hydrogel architecture ensures reliable contact between the electrolyte and the electrode. The composite hydrogel has the advantage of being able to function as binder-free supercapacitor electrodes, making it a feasible option for high-performance, low-cost energy storage devices. For both sides of the included ionic hydrogel electrolyte, *in situ* deposited PANI/graphene oxide nanocomposites were used to assemble an all-in-one integrated supercapacitor (AISC) by Ren *et al.*<sup>84</sup> The AISC assembly process was considerably simplified, and mechanical deformation did not result in the displacement or separation of the multilayer structured hydrogel complex. The ionic additives in the hydrogel electrolyte provided strong adhesion and flexibility, as well as high ionic conductivity, ensuring the AISC's superior specific capacitance and rate performance. A reactive shaping process

with two phases was used to create an inherently stretchy PANI hybrid hydrogel (PHH) by Yue *et al.*<sup>85</sup> The resultant PHH synthesised showed high stretchability and fatigue resistance due to the development of reversible hydrogen bonds and electrostatic interactions between the PAA/PEO and PANI networks. The reactive shaping process allowed for 3D reactive printing of PHH into pre-designed micro-lattice structures with high elasticity and electron/ion dual-conducting pathways, making it suitable for capacitive pressure sensors.

**1.4.5 Microbial fuel cells.** *In situ* polymerization was used to create a self-supporting PANI/sodium alginate/carbon brush (PANI-SA/CB) hydrogel as a material for microbial fuel cells (MFC anode) by Wang *et al.*<sup>86</sup> The PANI-SA-conducting hydrogels, which were simple to make, showed considerable promise as MFC anode electrode materials, Fig. 7.

A simple hydrothermal reaction was used to create a new three-dimensional ternary composite graphene-based hydrogel by Jayakumar and co-workers.<sup>87</sup> PGM-HCl, a graphene/PANI/ $\text{MnO}_x$  hydrogel obtained by controlling the morphology of  $\text{MnO}_x$  in an acidic environment using hydrochloric acid (HCl), had an extremely high specific capacitance of  $955 \text{ F g}^{-1}$  at a current density of  $1 \text{ A g}^{-1}$  and a capacitance retention of 89% after 1000 cycles and 69.1% after 5000 cycles at  $20 \text{ A g}^{-1}$ . Supramolecular self-assembly was used to make a PANI/poly(styrene sulfonate) (PSS) hydrogel with high concentrations of aniline (An) and PSS by Jia *et al.*<sup>88</sup> Pt supported on the PANI-PSS hydrogel exhibited better electrocatalytic activity towards the oxidation of methanol than Pt supported on the

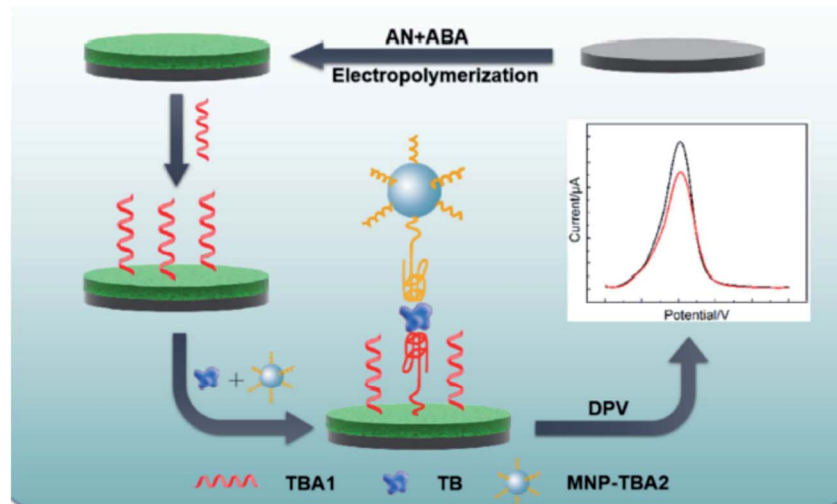


Fig. 7 Schematic illustration of antifouling electrochemical aptasensor working principle. (Reprinted with permission from Elsevier, ref. 86 Wang et al. (2019)).

PAn-PSS colloid, according to cyclic voltammograms and chronoamperometric tests. As a result, PANI/PSS hydrogel-Pt could be a viable methanol catalyst in fuel cells. Stretchable and tough composite hydrogels of  $\text{Fe}_3\text{O}_4/\text{MoS}_2/\text{PANI}$  with conductive and magnetic characteristics was synthesized by Hu *et al.*<sup>89</sup> A new bio-anode was built and electrically studied, incorporating gel-entrapped bacteria in alginate/PANI/TiO<sub>2</sub>/graphite composites by Szöllősi *et al.*<sup>90</sup> The microorganism cells were immobilised using alginate as a dopant and template, as well as an entrapped gel. The conductivity of gels increased as the concentration of PANI was increased. PANI at concentrations of 0.01 and 0.02 g mL<sup>-1</sup> showed increased conductivity by 6 and 10 times, respectively. By employing phytic acid as both a dopant and a cross-linking agent, a PANI hydrogel was created. The hydrogel was then used as an adsorbent to extract methylene blue (MB) from an aqueous solution by Yan *et al.*<sup>91</sup> To increase methane (CH<sub>4</sub>) production from anaerobic breakdown of organics in wastewater, a PANI hydrogel was utilised as the conductive medium by Zhou *et al.*<sup>92</sup> The anaerobe adherence was aided by the porous structure and hydrophilic surface of the PANI hydrogel. The constructed hydrogel demonstrated good biocompatibility with anaerobic bacteria.

## 2 Conclusion

CPHs are a special type of material that combines the benefits of both hydrogels and organic conductors. CPHs serve as an excellent interface between the electronic (electrode) and ionic (electrolyte) transporting phases, significantly improving electronic/ionic conductivity as well as reactivity to external stimuli. Integrity, strength, elasticity, and mechanical qualities are provided by composite type CPHs made up of insulating/supporting polymer networks. The combination of these qualities allows for a wide range of advanced applications in biomedical devices, bio-electrodes, bioelectronics, and other fields. Controlling the architecture of CPHs to tune

optoelectronic and bio-electronic properties is one of the unexplored topics in the field. Furthermore, the impact of conducting polymer functionality, redox nature, charge production, and biodegradability are all important considerations. The field of CPHs has a huge potential for extensive research into the structure–property correlations of these materials, and it has a promising future in terms of advanced green sustainable materials.

## Conflicts of interest

There are no conflicts to declare.

## Acknowledgements

AK acknowledges UGC-BSR (project no. F-30/569/2021 (BSR)) and DST-SERB (project no. SRG/2021/001709) for the financial assistant.

## References

- 1 S. K. Siddhanta and R. Gangopadhyay, *Polymer*, 2005, **46**, 2993–3000.
- 2 E. M. Ahmed, *J. Adv. Res.*, 2015, **6**, 105–121.
- 3 W. E. Roorda, H. E. Boddé, A. G. de Boer and H. E. Junginger, *Pharm. Weekbl.*, 1986, **8**, 165–189.
- 4 S. J. Buwalda, K. W. M. Boere, P. J. Dijkstra, J. Feijen, T. Vermonden and W. E. Hennink, *J. Controlled Release*, 2014, **190**, 254–273.
- 5 J. Melke, S. Midha, S. Ghosh, K. Ito and S. Hofmann, *Acta Biomater.*, 2016, **31**, 1–16.
- 6 R. Xing, K. Liu, T. Jiao, N. Zhang, K. Ma, R. Zhang, Q. Zou, G. Ma and X. Yan, *Adv. Mater.*, 2016, **28**, 3669–3676.
- 7 O. Chaudhuri, L. Gu, D. Klumpers, M. Darnell, S. A. Bencherif, J. C. Weaver, N. Huebsch, H. Lee,



E. Lippens, G. N. Duda and D. J. Mooney, *Nat. Mater.*, 2016, **15**, 326–334.

8 D. L. Taylor and M. in het Panhuis, *Adv. Mater.*, 2016, **28**, 9060–9093.

9 X. Zhao, H. Wu, B. Guo, R. Dong, Y. Qiu and P. X. Ma, *Biomaterials*, 2017, **122**, 34–47.

10 V. Yesilyurt, M. J. Webber, E. A. Appel, C. Godwin, R. Langer and D. G. Anderson, *Adv. Mater.*, 2016, **28**, 86–91.

11 R. Kumar, S. Ayyanar, P. Jayaraj, A. Sivaramakrishna, S. Rajagopalan, S. Parthasarathy and R. Desikan, *Hydrogel Formulation As Efficient Drug Carrier and Delivery for Selected Skin Diseases in Nano Hydrogels*, Springer, 2021, pp. 181–203.

12 F. Zhao, Y. Shi, L. Pan and G. Yu, *Acc. Chem. Res.*, 2017, **50**, 1734–1743.

13 H. Deng, L. Lin, M. Ji, S. Zhang, M. Yang and Q. Fu, *Prog. Polym. Sci.*, 2014, **39**, 627–655.

14 Y. Shi, L. Peng, Y. Ding, Y. Zhao and G. Yu, *Chem. Soc. Rev.*, 2015, **44**, 6684–6696.

15 Q. Rong, W. Lei and M. Liu, *Chem. - Eur. J.*, 2018, **24**, 16930–16943.

16 K. Sharma, V. Kumar, B. S. Kaith, S. Kalia and H. C. Swart, *Conducting Polymer Hydrogels and Their Applications, Part of the Springer Series on Polymer and Composite Materials book series (SSPCM)*, 2017, pp. 193–221.

17 R. D. Pyarasani, T. Jayaramudu and A. John, *J. Mater. Sci.*, 2019, **54**, 974–996.

18 I. Jeon, J. Cui, W. R. K. Illeperuma, J. Aizenberg and J. J. Vlassak, *Adv. Mater.*, 2016, **28**, 4678–4683.

19 H. Chen, F. Yang, Q. Chen and J. Zheng, *Adv. Mater.*, 2017, **29**, 1606900.

20 S. Ganguly, T. Maity, S. Mondal, P. Das and N. C. Das, *Int. J. Biol. Macromol.*, 2017, **95**, 185–198.

21 Y.-J. Liu, W.-T. Cao, M.-G. Ma and P. Wan, *ACS Appl. Mater. Interfaces*, 2017, **9**, 25559–25570.

22 V. V. Tran, D. Park and Y. C. Lee, *Environ. Sci. Pollut. Res.*, 2018, **25**, 24569–24599.

23 Y. Cheng, X. Ren, L. Duan and G. Gao, *J. Mater. Chem. C*, 2020, **8**, 8234–8242.

24 Z. Ma, W. Shi, K. Yan, L. Pan and G. Yu, *Chem. Sci.*, 2019, **10**, 6232–6244.

25 Y. Guo, J. Bae, F. Zhao and G. Yu, *Trends Green Chem.*, 2019, **1**, 335–348.

26 P. Sista, K. Ghosh, J. S. Martinez and R. C. Rocha, *J. Nanosci. Nanotechnol.*, 2014, **14**, 250–272.

27 A. B. Khiabani and M. Gasik, *J. Macromol. Chem.*, 2022, **23**(7), 3665.

28 A. R. Spencer, A. Primbetova, A. N. Koppes, R. A. Koppes, H. Fenniri and N. Annabi, *ACS Biomater. Sci. Eng.*, 2018, **4**(5), 1558–1567.

29 U. Riaz, N. Singh, F. Rashnas Srabikal and S. Fatima, *Polym. Bull.*, 2022, DOI: [10.1007/s00289-022-04120-6](https://doi.org/10.1007/s00289-022-04120-6).

30 S. Mondal, U. Rana and S. Malik, *Chem. Commun.*, 2015, **51**, 12365–12368.

31 S. Mondal, U. Rana and S. Malik, *ACS Appl. Mater. Interfaces*, 2015, **7**, 10457–10465.

32 S. Mondal, U. Rana, R. R. Bhattacharjee and S. Malik, *RSC Adv.*, 2014, **4**, 57282–57289.

33 S. Mondal and S. Malik, *J. Power Sources*, 2016, **328**, 271–279.

34 S. Mondal, U. Rana and S. Malik, *J. Phys. Chem. C*, 2017, **121**, 7573–7583.

35 M. V. Martínez, S. Bongiovanni Abel, R. Rivero, M. C. Miras, C. R. Rivarola and C. A. Barbero, *Polymer*, 2015, **78**, 94–103.

36 M. A. Molina, C. R. Rivarola, M. C. Miras, D. Lescano and C. A. Barbero, *Nanotechnology*, 2011, **22**, 245504.

37 M. A. Molina, C. R. Rivarola and C. A. Barbero, *Eur. Polym. J.*, 2011, **47**, 1977–1984.

38 Y. Wu, Y. X. Chen, J. Yan, S. Yang, P. Dong and P. Soman, *J. Mater. Chem. B*, 2015, **3**, 5352–5360.

39 H. Huang, X. Zeng, W. Li, H. Wang, Q. Wang and Y. Yang, *J. Mater. Chem. A*, 2014, **2**, 16516–16522.

40 M. Nourbakhsh, P. Zarrintaj, S. H. Jafari, S. M. Hosseini, S. Aliakbari, H. G. Pourbadie, N. Naderi, M. I. Zibaii, S. S. Gholizadeh, J. D. Ramsey, S. Thomas, M. Farokhi and M. R. Saeb, *Mater. Sci. Eng., C*, 2020, **117**, 111328.

41 S. U. Rahman, S. Bilal and A. ul Haq Ali Shah, *Polymers*, 2020, **12**, 2870.

42 X. Zhao, P. Li, B. Guo and P. X. Ma, *Acta Biomater.*, 2015, **26**, 236–248.

43 K. Sharma, B. S. Kaith, V. Kumar, S. Kalia, V. Kumar and H. C. Swart, *Polym. Degrad. Stab.*, 2014, **107**, 166–177.

44 T. Dai, X. Qing, J. Wang, C. Shen and Y. Lu, *Compos. Sci. Technol.*, 2010, **70**, 498–503.

45 J. Jia, R. Li, H. Li, Y. Shu, Y. Li, S. Qiu, C. He and Y. Yang, *Composites, Part B*, 2018, **155**, 132–137.

46 M. A. Smirnov, M. P. Sokolova, N. V. Bobrova, I. A. Kasatkin, E. Lahderanta and G. K. Elyashevich, *J. Power Sources*, 2016, **304**, 102–110.

47 H. Ding, M. Zhong, Y. J. Kim, P. Pholpabu, A. Balasubramanian, C. M. Hui, H. He, H. Yang, K. Matyjaszewski and C. J. Bettinger, *ACS Nano*, 2014, **8**, 4348–4357.

48 P. Marcauszaa, S. Reynaud, F. Ehrenfeld, A. Khoukh and J. Desbrieres, *Biomacromolecules*, 2010, **11**, 1684–1691.

49 V. Guarino, M. A. Alvarez-Perez, A. Borriello, T. Napolitano and L. Ambrosio, *Adv. Healthcare Mater.*, 2013, **2**, 218–227.

50 Z. Yang, A. Qiu, J. Ma and M. Chen, *Compos. Sci. Technol.*, 2018, **156**, 231–237.

51 B. C. Nath, B. Gogoi, M. Boruah, S. Sharma, M. Khannam, G. A. Ahmed and S. K. Dolui, *Electrochim. Acta*, 2014, **146**, 106–111.

52 Z. Liu, A. Lu, Z. Yang and Y. Luo, *Macromol. Res.*, 2013, **21**, 376–384.

53 J. Wang, B. Li, T. Ni, T. Dai and Y. Lu, *Compos. Sci. Technol.*, 2015, **109**, 12–17.

54 B. Taşdelen, *Mater. Today: Proc.*, 2018, **5**, 15983–15989.

55 K. Depa, A. Strachota, M. Šlouf, J. Brus and V. Cimrová, *Sens. Actuators, B*, 2017, **244**, 616–634.

56 Y. Zhang, S. Xie, D. Zhang, B. Ren, Y. Liu, L. Tang, Q. Chen, J. Yang, J. Wu, J. Tang and J. Zheng, *Eng. Sci.*, 2019, **6**, 1–11, DOI: [10.30919/es8d788](https://doi.org/10.30919/es8d788).



57 P. Y. Chen, N.-M. Dorval Courchesne, M. N. Hyder, J. Qi, A. M. Belcher and P. T. Hammond, *RSC Adv.*, 2015, **5**, 37970–37977.

58 I. Y. Dmitriev, P. V. Vlasov, M. F. Lebedeva, I. V. Gofman, V. Y. Elokhovsky, E. N. Popova, M. S. Lozhkin, E. N. Vlasova, I. S. Kuryndin, M. A. Smirnov and G. K. Elyashevich, *Mater. Chem. Phys.*, 2017, **187**, 88–95.

59 L. M. Lira and S. I. Córdoba de Torresi, *Electrochim. Commun.*, 2005, **7**, 717–723.

60 K. Wang, X. Zhang, C. Li, H. Zhang, X. Sun, N. Xu and Y. Ma, *J. Mater. Chem. A*, 2014, **2**, 19726–19732.

61 X. Chu, H. Huang, H. Zhang, H. Zhang, B. Gu, H. Su, F. Liu, Y. Han, Z. Wang, N. Chen, C. Yan, W. Deng, W. Deng and W. Yang, *Electrochim. Acta*, 2019, **301**, 136–144.

62 D. Zhai, B. Liu, Y. Shi, L. Pan, Y. Wang, W. Li, R. Zhang and G. Yu, *ACS Nano*, 2013, **7**, 3540–3546.

63 S. Zeng, H. Chen, F. Cai, Y. Kang, M. Chen and Q. Li, *J. Mater. Chem. A*, 2015, **3**, 23864–23870.

64 S. Gao, L. Zhang, Y. Qiao, P. Dong, J. Shi and S. Cao, *RSC Adv.*, 2016, **6**, 58854–58861.

65 S. Adhikari and P. Banerji, *Synth. Met.*, 2009, **159**, 2519–2524.

66 F. A. Aouada, M. R. de Moura, P. R. G. Fernandes, A. F. Rubira and E. C. Muniz, *Eur. Polym. J.*, 2005, **41**, 2134–2141.

67 M. El Fray, A. Pilaszkiewicz, W. Swieszkowski and K. J. Kurzydlowski, *Eur. Polym. J.*, 2007, **43**, 2035–2040.

68 L. Li, J. Ge, P. X. Ma and B. Guo, *RSC Adv.*, 2015, **5**, 92490–92498.

69 R. Komeri and J. Muthu, *Colloids Surf., B*, 2017, **157**, 381–390.

70 X. Wang, F. Gao, Y. Gong, G. Liu, Y. Zhang and C. Ding, *Talanta*, 2019, **205**, 120140.

71 L. Yang, H. Wang, H. Lü and N. Hui, *Anal. Chim. Acta*, 2020, **1124**, 104–112.

72 M. Qing, S. L. Chen, L. Han, Y. Z. Yang, H. Q. Luo and N. B. Li, *Biosens. Bioelectron.*, 2020, **158**, 112179.

73 J. Han, Q. Ding, C. Mei, Q. Wu, Y. Yue and X. Xu, *Electrochim. Acta*, 2019, **318**, 660–672.

74 L. Zhao and Z. Ma, *Anal. Chim. Acta*, 2018, **997**, 60–66.

75 K. Sharma, V. Kumar, B. Chaudhary, B. S. Kaith, S. Kalia and H. C. Swart, *Polym. Degrad. Stab.*, 2016, **124**, 101–111.

76 A. Pourjavadi and M. Doroudian, *Polymer*, 2015, **76**, 287–294.

77 J. Qu, X. Zhao, P. X. Ma and B. Guo, *Acta Biomater.*, 2018, **72**, 55–69.

78 T.-S. Tsai, V. Pillay, Y. E. Choonara, L. C. Du Toit, G. Modi, D. Naidoo and P. Kumar, *Polymers*, 2011, **3**, 150–172.

79 X. Fu, T. Li, F. Qi, S. Zhang, J. Wen, W. Shu, P. Luo, R. Zhang, S. Hu and Q. Liu, *Appl. Surf. Sci.*, 2020, **507**, 145135.

80 Y. Jia, J. Jiang, K. Sun and T. Dai, *J. Appl. Polym. Sci.*, 2012, **125**, 3702–3707.

81 S. Cao, T. Zhao, Y. Li, L. Yang, A. Ahmad, T. Jiang, Y. Shu, Z. Jing, H. Luo, X. Lu and H. Zhang, *Ceram. Int.*, 2022, **48**, 15721–15728.

82 S. Sardana, A. Gupta, A. S. Maan, S. Dahiya, K. Singh and A. Ohlan, *Indian J. Phys.*, 2022, **96**, 433–439.

83 S. Sardana, K. Aggarwal, P. Siwach, L. Gaba, A. S. Maan, K. Singh and A. Ohlan, *Energy Storage*, DOI: [10.1002/est2.328](https://doi.org/10.1002/est2.328).

84 Y. Ren, C. Sun, Y. Liu, Y. Hong, Q. Wang, W. Zhao, S. Li, W. Wang and X. Dong, *Sci. China Mater.*, 2022, **65**, 373–382.

85 M. Yue, Y. Wang, H. Guo, C. Zhang and T. Liu, *Compos. Sci. Technol.*, 2022, **220**, 109263.

86 Y. Wang, Q. Wen, Y. Chen, H. Zheng and S. Wang, *Energy*, 2020, **202**, 117780.

87 A. Jayakumar, Y.-J. Yoon, R. Wang and J.-M. Lee, *RSC Adv.*, 2015, **5**, 94388–94396.

88 Q. Jia, C. Yang, Q. Pan, Y. Xin, F. Xu, W. Qi, H. Wei, S. Yang, C. Zhou, N. Hu and B. Cao, *Chem. Eng. J.*, 2020, **383**, 123153.

89 H. Hu, X. Zhong, S. Yang and H. Fu, *Composites, Part B*, 2020, **182**, 107623.

90 A. Szöllősi, Á. Hoschke, J. M. Rezessy-Szabó, E. Bujna, S. Kun and Q. D. Nguyen, *Chemosphere*, 2017, **174**, 58–65.

91 B. Yan, Z. Chen, L. Cai, Z. Chen, J. Fu and Q. Xu, *Appl. Surf. Sci.*, 2015, **356**, 39–47.

92 N. Zhou, T. Wang, S. Chen, Q. Hu, X. Cheng, D. Sun, S. Vupputuri, B. Qiu, H. Liu and Z. Guo, *J. Colloid Interface Sci.*, 2021, **581**, 314–322.

